Optics Letters

Femtosecond laser line-by-line inscription of apodized fiber Bragg gratings

JUN HE,[1,2] ZIYONG CHEN,[1,2] XIZHEN XU,[1,2,*] JIA HE,[1,2] BAIJIE XU,[1,2] BIN DU,[1,2] KUIKUI GUO,[1,2] RUNXIAO CHEN,[1,2] AND YIPING WANG[1,2]

[1]Key Laboratory of Optoelectronic Devices and Systems of Ministry of Education/Guangdong Province, College of Physics and Optoelectronic Engineering, Shenzhen University, Shenzhen 518060, China
[2]Shenzhen Key Laboratory of Photonic Devices and Sensing Systems for Internet of Things, Guangdong and Hong Kong Joint Research Centre for Optical Fibre Sensors, Shenzhen University, Shenzhen 518060, China
*Corresponding author: xizhenxu@szu.edu.cn

Received 30 August 2021; revised 12 October 2021; accepted 22 October 2021; posted 26 October 2021 (Doc. ID 441888); published 9 November 2021

The reflection spectra of conventional fiber Bragg gratings (FBGs) with uniform index modulation profiles typically have strong sidelobes, which hamper the performance of FBG-based optical filters, fiber lasers, and sensors. Here, we propose and demonstrate a femtosecond laser line-by-line (LbL) scanning technique for fabricating apodized FBGs with suppressed sidelobes. This approach can flexibly achieve various apodized modulation profiles via precise control over the length and/or transverse position of each laser-inscribed index modification track. We theoretically and experimentally studied the influences of the apodization function on the side-mode suppression ratio (SMSR) in the fabricated apodized FBG, and the results show that a maximum SMSR of 20.6 dB was achieved in a Gaussian-apodized FBG. Subsequently, we used this method to fabricate various apodized FBGs, and the SMSRs in these FBGs were reduced effectively. Specifically, a dense-wavelength-division-multiplexed Gaussian-apodized FBG array with a wavelength interval of 1.50 nm was successfully fabricated, and the SMSR in such an array is 14 dB. Moreover, a Gaussian-apodized phase-shifted FBG and chirped FBG were also demonstrated with a high SMSR of 14 and 16 dB, respectively. Therefore, such an apodization method based on a modified femtosecond laser LbL scanning technique is an effective and flexible way to fabricate various FBGs with high SMSRs, which is promising to improve the performance of optical filters, fiber lasers, and sensors.

https://doi.org/10.1364/OL.441888

Fiber Bragg gratings (FBGs) have received much attention as optical filters, reflectors, and sensing elements in many areas, such as dense-wavelength-division-multiplexed (DWDM) transmission systems, high-performance fiber-optic sensing systems, and fiber lasers [1–4]. However, the typical sidelobes in uniform FBG spectra can be problematic for applications, resulting in cross talk in DWDM systems, instabilities in Q-switched fiber lasers, and linewidth broadening in high-power fiber lasers [5,6]. Conventionally, FBGs are generated by using a UV laser phase mask method. To date, various apodized approaches based on the UV laser and the phase mask have been proposed for suppressing the unwanted side mode. For example, a phase mask with variable diffraction efficiencies was employed to fabricate apodized FBGs [7]. Some apodized methods require only a conventional phase mask. They include phase mask dithering, scanning phase mask method with modification of exposure time, double-UV-exposure method, and polarization control of the UV beam [8–11]. Nevertheless, UV laser-induced FBGs can withstand a limited operation temperature of merely 450°C [12]. In 2003, Mihailov *et al.* reported the fabrication of FBGs by using a femtosecond laser phase mask method [13]. They demonstrated that femtosecond laser-induced FBGs exhibit excellent thermal stability (up to 1000°C) [14]. Since then, various techniques based on phase masks have been proposed to write special FBGs. For example, chirped FBGs can be obtained by using such two methods, i.e., a thermally tunable phase mask and variable wavefront tuning based on a spatial light modulator [15,16]. A strain-assisted method was proposed to inscribe phase-shifted FBGs and FBG arrays [17,18].

Moreover, femtosecond laser direct writing techniques, such as point-by-point (PbP) and line-by-line (LbL) methods, have been reported and used for fabricating FBGs [19,20]. These techniques exhibit excellent flexibility in control over the position of each refractive index modulation (RIM), favoring the creation of FBGs with complex index profiles, such as apodized FBGs, chirped FBGs, and phase-shifted FBGs [21–25]. For example, the femtosecond laser PbP method was proposed to fabricate apodized FBGs through precise control over the transverse position of each laser-inscribed RIM, thereby varying the overlap of the RIM with the core mode [22,23]. Moreover, apodized Bragg grating waveguides were created successfully by the PbP method, exhibiting excellent flexibility in fabrication of highly integrated 3D optical circuits [24]. However, the small RIM area can be formed by a single laser pulse. Such a PbP method is unsuitable for fabricating highly reflective FBGs in large-mode-area fibers. The femtosecond laser LbL method was demonstrated to enlarge the RIM area effectively.

Such a method has been proposed to fabricate regular FBGs, phase-shifted FBGs, and chirped FBGs [20,25].

In this Letter, we report on a new method for fabricating apodized FBGs with a modified femtosecond laser LbL scanning technique. The apodization approach is to tailor the local coupling amplitude of the gratings through precise control over the track length or transverse position of each laser-inscribed RIM, thereby changing the overlap of the RIM with the fiber core mode. We studied FBGs with various apodization profiles, such as cosine, linear, and Gaussian functions. The experimental and simulation results show that the Gaussian-apodized FBG exhibits a maximum side-mode suppression ratio (SMSR). Moreover, a DWDM Gaussian-apodized FBG array with a wavelength interval of 1.50 nm was successfully constructed, and the sidelobes were suppressed effectively. In addition, a phase-shifted FBG and a chirped FBG with a high SMSR were fabricated by using a Gaussian apodization function. These results show that such an apodization approach is suitable for improving the SMSR in various FBGs.

The schematics of the inscription of apodized FBGs are exhibited in Fig. 1, in which we employ a frequency-doubled regenerative amplified Yb:KGW ($KGd(WO_3)$) femtosecond laser (Pharos, Light-conversion) with a central wavelength of 514 nm, pulse width of 290 fs, repetition rate of 200 kHz, and laser spot diameter of 3 mm. Second-order FBGs were fabricated in single mode silica fiber (SMF, corning SMF-28e) with target wavelengths in the range of 1520–1570 nm (corresponding to periods of approximately ~1 μm). A Zeiss oil-immersion objective [63×, numerical aperture (NA) = 1.40] was selected in the experiment. Moreover, the fiber was fixed on an assembled 3D air-bearing translation stage (Aerotech ABL15010, 107 ANT130LZS, and ANT130V-5) so that the desired pattern could be written by translating the fiber with respect to the focal spot of the femtosecond laser beam. The gap between the objective and SMF were filled with index matching oil to eliminate the distortion induced by the fiber cylindrical surface. In the fabrication process, FBGs are inscribed through coating directly.

Subsequently, in the case in which the femtosecond laser beam was focused into the fiber, the LbL scanning process was implemented by simultaneously controlling the assembled 3D air-bearing translation stage and a shutter. As a result, a Bragg

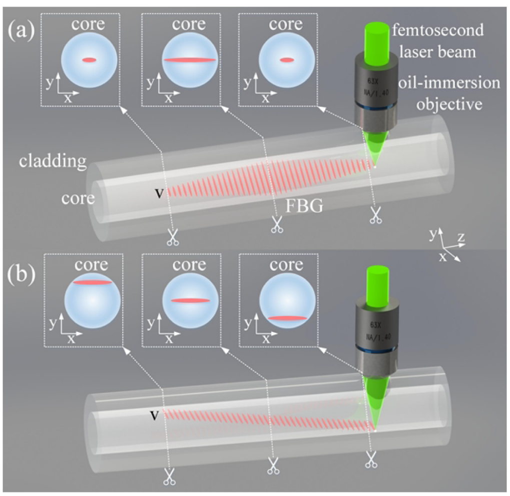

Fig. 1. Schematics of two femtosecond laser line-by-line inscription methods for creating apodized FBGs by (a) controlling the track length and (b) controlling the track position.

grating with a grating pitch of Λ, track length of b, and pitch quantity of N was formed by these tracks inscribed in a fiber core. In this process, the translation speed v and the pulse energy were set to be 0.2 mm/s and 10 nJ, respectively. Moreover, we propose two methods, i.e., precise control over the length or transverse position of these tracks, to achieve apodized profiles by using the LbL scanning technique, as shown in Figs. 1(a) and 1(b).

The intensity profile of the fiber core mode is approximately Gaussian, and the axial length of the focal volume (1 μm) is small with respect to the $1/e^2$ width of the guided mode (10 μm). It follows that the laser-inscribed track with various lengths can be induced over the transverse position precisely and flexibly. Hence, the overlap of the RIM with the core mode can be adjusted by controlling the size and position of the RIM, and tailoring the local coupling strength. As shown in Fig. 1(a), the overlap factor η is determined to be [26]

$$\eta(b) = 1 - \exp(-2a \cdot b(z)/\pi w^2), \tag{1}$$

where a and w are the height of the laser-induced track and the mode field radius, respectively. The length of the laser-induced track $b(z)$ is a function of the position of the fiber axis. For a given RIM Δn, the coupling strength κ depends on the relative overlap $\eta(b)$ between the fundamental propagation mode in the fiber and extent of the refractive index planes of the grating:

$$\kappa(\eta) = \frac{\eta(b)\pi\Delta n}{\lambda_B}, \tag{2}$$

where λ_B is the Bragg wavelength. Thus, the desired apodization profile is achieved by combining a function $\eta(b)$ that defines the absolute value of the coupling strength κ.

As shown in Fig. 1(b), the laser-induced tracks have the same length, leading to the constant overlap factor η. Through the Gaussian form of the guided mode, the actual local coupling strength κ in these LbL gratings is dependent on the offset of the RIMs from the center of the core according to [22]

$$\kappa(z) = \kappa_0 \exp[-(4y(z)/w)^2], \tag{3}$$

where κ_0 is the coupling strength caused by the RIM located at the center of the fiber core.

The transfer matrix method was used to analyze the spectral characteristics of apodized FBGs [26]. A numerical solution of the reflection spectrum of the apodized FBG can be evaluated by using MATLAB.

First, we fabricated a uniform FBG (i.e., S1) and three apodized FBGs (i.e., S2–S4). These FBG samples have the same grating pitch of 1.070 μm and the same grating length of 2 mm. Note that the track lengths $b(z)$ of S2–S4 vary as cosine, linear, and Gaussian functions of the position of the fiber axis, respectively. As shown in Figs. 2(a1)–2(a4), S1 has a uniform track length of 10 μm in the entire grating, while S2–S4 have varied track lengths obviously. Reflection spectra of four samples were measured using a 1 × 2, 3 dB fiber coupler (Golight, fiber type: SMF-28e, coupling ratio: 50:50) connecting a broadband light source with a wavelength range from 1250 to 1650 nm (Fiber Lake, ASE-LIGHT SOURCE) and an optical spectrum analyzer (OSA, YOKOGAWA AQ6370D). The scanning span ranged from 1520 to 1580 nm. The resolution and the sampling were 0.05 nm and 6001, respectively. As displayed in Figs. 2(b1)–2(b4), S1–S4 have a Bragg wavelength

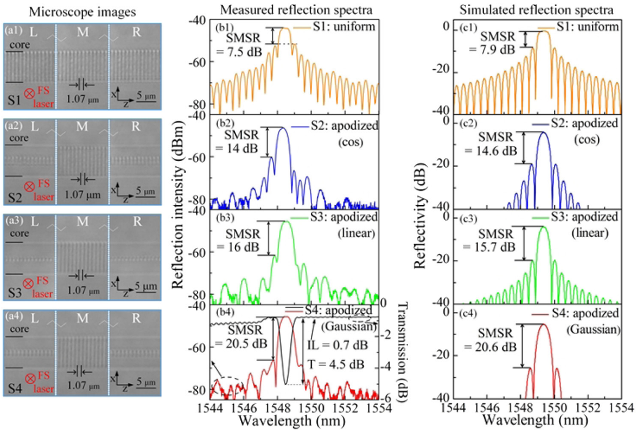

Fig. 2. Uniform FBG S1 and three apodized FBGs S2–S4 with different modulation profiles (i.e., cosine, linear, and Gaussian functions) inscribed by controlling the track length. (a) Lateral-view microscope images; (b) measured reflection spectra and transmission spectrum of S4; (c) simulated reflection spectra.

of 1549.50 nm. It can be found from Fig. 2(b1) that S1 has a minimum SMSR of 7.5 dB, and the simulated reflection spectrum, as shown in Fig. 2(c1), exhibits a similar SMSR of 7.9 dB. In the case of S2 (cosine-adopized FBG), as shown in Fig. 2(b2), an improved SMSR of 14 dB can be achieved, which agrees well with the simulated results as shown in Fig. 2(c2). Moreover, in the case of S3 (linear-adopized FBG), as shown in Fig. 2(b3), the SMSR is improved further to 16 dB and the simulated reflection spectrum, as shown in Fig. 2(c3), exhibits the same trend. Then, in the case of S4 (Gaussian-adopized FBG), as shown in Fig. 2(b4), the side modes are suppressed significantly, and a maximum SMSR of 20.5 dB can be obtained, which is in good agreement with the simulated results, as shown in Fig. 2(c4). Moreover, the transmission spectrum of this sample exhibits an insertion loss of 0.7 dB and the Bragg resonance attenuation of 4.5 dB (i.e., reflectivity of 66.4%). Hence, in the case of controlling the length of tracks, an apodized FBG with a SMSR of up to 20 dB was successfully created by using an appropriate apodized function (i.e., Gaussian function).

Subsequently, we fabricated three more apodized FBGs (i.e., S5–S7), and these samples have the same grating pitch of 1.070 μm, the same track length of 10 μm, and the same grating length of 2 mm. Note that the offset $y(z)$ of the track from the center of the core in S5–S7 varies as cosine, linear, and Gaussian functions of the position of the fiber axis, respectively. As shown in Fig. 3(a), all of the tracks in these samples have a uniform axial length of focal volume (i.e., 3 μm). Moreover, the offset $y(z)$ is maximum at the front and end of the grating, and the track is located at the center of the core in the middle of the entire grating. Then, as shown in Figs. 3(b1)–3(b3), the reflection spectra of S5–S7 exhibit SMSRs of 16, 16, and 17 dB, respectively, and the simulation results agree well with the measurement results, as shown in Figs. 3(c1)–3(c3). Consequently, in the case of controlling the position of the track, the Gaussian apodized FBG has the maximum SMSR. The results demonstrate that an enhanced SMSR of up to 20 dB can be achieved by controlling the lengths of tracks and using the appropriate apodized function (i.e., Gaussian function).

Moreover, we investigated the effect of the apodization approach on the reflection spectrum of a DWDM FBG array.

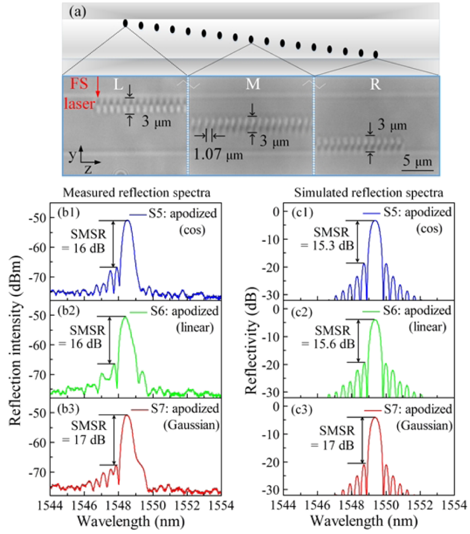

Fig. 3. Three apodized FBGs S5–S7 with different modulation profiles (i.e., cosine, linear, and Gaussian functions) inscribed by controlling the track position. (a) Lateral-view microscope images; (b) measured reflection spectra; (c) simulated reflection spectra.

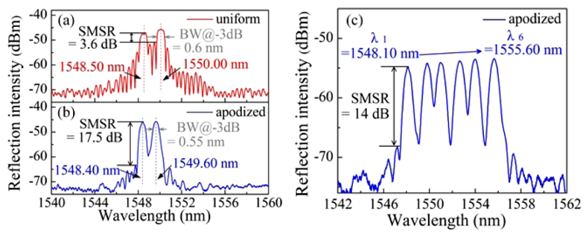

Fig. 4. Reflection spectra of three DWDM FBG arrays consisting of (a) two uniform FBGs, (b) two apodized FBGs, and (c) six apodized FBGs.

First, we fabricated a DWDM FBG array consisting of two uniform FBGs with a grating length of 2 mm. The pitches were 1.070 and 1.071 μm. Subsequently, another Gaussian-apodized FBG array was created with the same fabricated parameters by controlling the track lengths. As shown in Fig. 4(a), the corresponding Bragg wavelengths of two uniform FBGs are 1548.50 and 1550.00 nm, respectively, and the −3 dB bandwidth is 0.6 nm. It can be found that the SMSR of 3.6 dB can be achieved merely in the reflection spectrum of such a uniform FBG array. Then, in the case of the DWDM Gaussian-apodized FBG array, the reflection spectrum has an improved SMSR of 17.5 dB, as shown in Fig. 4(b). Moreover, the Bragg wavelengths are 1548.40 and 1549.60 nm, respectively, and the bandwidth is 0.55 nm. In addition, we fabricated a DWDM Gaussian-apodized FBG array including six FBGs with a grating length of 2 mm. The pitches are 1.07, 1.071, 1.072, 1.073, 1.074, and 1.075 μm, and the corresponding Bragg wavelengths are 1548.10, 1549.59, 1550.98, 1552.67, and 1555.60 nm, respectively. As illustrated in Fig. 4(c), the reflection spectrum exhibits a SMSR of 14 dB. The results indicate that such an apodization approach can be effective to improve the SMSR of the DWDM FBG array.

Furthermore, we fabricated a phase-shifted FBG and a chirped FBG by employing the Gaussian apodized function. In the case of a phase-shifted FBG, the pitch and grating length

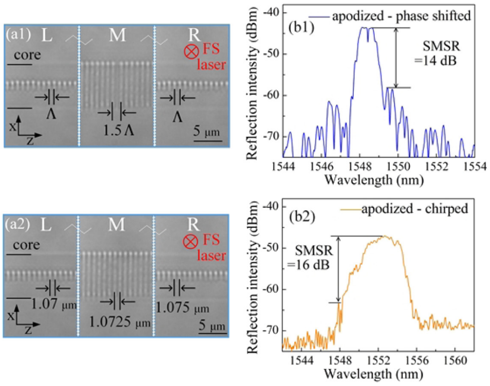

Fig. 5. (a) Lateral-view microscope images and (b) reflection spectra of apodized phased-shifted FBG and apodized chirped FBG.

are 1.07 μm and 4 mm, respectively, and the designed phase value of π is located in the middle of the grating, as shown in Fig. 5(a1). The reflection spectrum of such a sample, as displayed in Fig. 5(b1), exhibits a SMSR of 14 dB, which demonstrates that such an apodization approach can be used to improve the SMSR of phase-shifted FBGs. Additionally, we use $n+1$ grating fragments to construct a step-chirped FBG. Each grating fragment has a uniform pitch Λ, and the pitch of grating fragments increases linearly with steps of $d\Lambda$, producing pitches of Λ, $\Lambda + d\Lambda \ldots$, and $\Lambda + n \times d\Lambda$. Parameters were set as follows: $\Lambda = 1.07$ μm, $n = 62$, and $d\Lambda = 0.08$ nm, which was the minimum sensitivity for the translation stage, and the grating length of 4 mm was achieved. Figure 5(a2) shows that the pitch increases from 1.07 to 1.075 μm along the entire FBG. As displayed in Fig. 5(b2), the sidelobes in the reflection spectrum are suppressed obviously. Moreover, a broad reflection peak with a bandwidth of 3.6 nm and a SMSR of 16 dB is achieved. This result demonstrates that the SMSR of the chirped FBG can be improved effectively using such an apodized approach.

In summary, we have demonstrated two flexible methods for the fabrication of apodized FBGs based on a modified femtosecond laser LbL scanning technique, i.e., by controlling the track length and/or by controlling the track position. Effects of the apodization function on the SMSRs of FBGs were investigated. Moreover the simulation results and the measurement results show that the Gaussian apodized FBG exhibits a maximum SMSR of up to 20 dB. Subsequently, a DWDM Gaussian-apodized FBG array was successfully fabricated, and the reflection spectrum shows that the sidelobes of FBGs are suppressed obviously. In addition, the Gaussian apodization function was used to create a phase-shifted FBG and a chirped FBG. These two samples have enhanced SMSRs of 14 and 16 dB, respectively. As a result, the proposed apodization approach based on the femtosecond laser LbL scanning technique is very suitable for production of FBGs with high SMSRs, which is promising to improve the performance of optical filters, fiber lasers, and sensors.

Funding. National Natural Science Foundation of China (U1913212, 61875128, 62005170); Guangdong Science and Technology Department (2019TQ05X113, 2019A1515011393, 2019A1515111114); Shenzhen Science and Technology Innovation Program (RCYX20200714114538160, JCYJ20180507182058432, JCYJ20200109114201731).

Disclosures. The authors declare no conflicts of interest.

Data Availability. Data underlying the results presented in this paper are not publicly available at this time but may be obtained from the authors upon reasonable request.

REFERENCES

1. J. Madrigal, F. J. F. Peláez, D. Zheng, D. Barrera, and S. Sales, Opt. Express **25**, 24650 (2017).
2. Y. Wang, S. Y. Xiang, B. Wang, X. Y. Cao, A. J. Wen, and Y. Hao, Opt. Express **27**, 8446 (2019).
3. N. A. Mohammed, T. A. Ali, and M. H. Aly, AIP Adv. **3**, 122125 (2013).
4. N. A. Mohammed and H. O. E. Serafy, Appl. Opt. **57**, 273 (2018).
5. X. P. Cheng, J. Zhang, P. Shum, M. Tang, and R. F. Wu, IEEE Photon. Technol. Lett. **19**, 1646 (2007).
6. N. Jovanovic, M. Aslund, A. Fuerbach, S. D. Jackson, G. D. Marshall, and M. J. Withford, Opt. Lett. **32**, 2804 (2007).
7. J. Albert, K. O. Hill, B. Malo, S. Thériault, F. Bilodeau, D. C. Johnson, and L. E. Erickson, Electron. Lett. **31**, 222 (1995).
8. H. F. Qi, Z. Q. Song, S. J. Li, J. Guo, C. Wang, and G. D. Peng, Opt. Express **21**, 11309 (2013).
9. T. Osuch, P. Gasior, and L. Lewandowski, Proc. SPIE **5775**, 222 (2005).
10. Z. Q. Lin, X. F. Chen, F. Wu, J. S. Shi, Y. Z. Yin, and S. Z. Xie, Opt. Laser Technol. **35**, 315 (2003).
11. K. P. Chuang, Y. Lai, and L. G. Sheu, Opt. Lett. **29**, 340 (2004).
12. J. He, B. J. Xu, X. Z. Xu, C. R. Liao, and Y. P. Wang, Photon. Sens. **11**, 203 (2021).
13. S. J. Mihailov, C. W. Smelser, P. Lu, R. B. Walker, D. Grobnic, H. Ding, and J. Unruh, Opt. Lett. **28**, 995 (2003).
14. D. Grobnic, C. W. Smelser, S. J. Mihailov, and R. B. Walker, Meas. Sci. Technol. **17**, 1009 (2006).
15. C. Voigtländer, J. Thomas, E. Wikszak, P. Dannberg, S. Nolte, and A. Tünnermann, Opt. Lett. **34**, 1888 (2009).
16. C. Voigtländer, R. G. Krämer, T. A. Goebel, D. Richter, and S. Nolte, Opt. Lett. **41**, 17 (2016).
17. A. Halstuch and A. A. Ishaaya, Opt. Lett. **43**, 3893 (2018).
18. J. Habel, T. Boilard, J. S. Frenière, F. Trépanier, and M. Bernier, Sensors **17**, 2519 (2017).
19. A. Martinez, M. Dubov, I. Khrushchev, and I. Bennion, Electron. Lett. **40**, 1170 (2004).
20. K. M. Zhou, M. Dubov, C. B. Mou, L. Zhang, V. K. Mezentsev, and I. Bennion, IEEE Photon. Technol. Lett. **22**, 1190 (2010).
21. G. D. Marshall, R. J. Williams, N. Jovanovic, M. J. Steel, and M. J. Withford, Opt. Express **18**, 19844 (2010).
22. R. J. Williams, C. Voigtländer, G. D. Marshall, A. Tünnermann, S. Nolte, M. J. Steel, and M. J. Withford, Opt. Lett. **36**, 2988 (2011).
23. R. J. Williams, R. G. Krämer, S. Nolte, M. J. Withford, and M. J. Steel, Opt. Express **21**, 26854 (2013).
24. P. Zeil, C. Voigtländer, J. Thomas, D. Richter, and S. Nolte, Opt. Lett. **38**, 2354 (2013).
25. K. M. Yang, C. R. Liao, S. Liu, J. He, J. Wang, and Y. P. Wang, J. Lightwave Technol. **38**, 1474 (2020).
26. G. A. Cranch and G. M. H. Flockhart, J. Mod. Opt. **59**, 493 (2012).